Agricultural Systems xxx (2016) xxx–xxx

Contents lists available at ScienceDirect

Agricultural Systems

journal homepage: www.elsevier.com/locate/agsy

Distinguishing between endogenous and exogenous price volatility in food security assessment: An empirical nonlinear dynamics approach

R. Huffaker [a,*], M. Canavari [b], R. Muñoz-Carpena [c]

[a] Department of Agricultural and Biological Engineering, University of Florida, 281 Frazier Rogers Hall, Gainesville, FL 32611-0570, USA
[b] Dipartimento di Scienze Agrarie, Alma Mater Studiorum-Università di Bologna, Viale Giuseppe Fanin, 50, 40127 Bologna, Italy
[c] Department of Agricultural and Biological Engineering, University of Florida, 287 Frazier Rogers Hall, Gainesville, FL 32611-0570, USA,

ARTICLE INFO

Article history:
Received 19 October 2015
Received in revised form 26 September 2016
Accepted 29 September 2016
Available online xxxx

Keywords:
Food security
Price volatility
Phase space reconstruction

ABSTRACT

We propose an empirical scheme—based on nonlinear dynamics—for diagnosing real-world market dynamics from observed price series data. The scheme distinguishes between endogenous and exogenous volatility in observed price series, tests whether endogenous volatility is generated by low-dimensional deterministic market dynamics, simulates these dynamics with a phenomenological market model, and models extreme volatility probabilistically. These diagnostics allow policymakers to make an empirically-informed determination of whether laissez-faire or interventionist policies are most promising in reducing price volatility in particular cases. We apply the diagnostic scheme to provide compelling empirical evidence that observed volatility in organic apple, pear, orange, and lemon prices at the Milano (Italy) Ipercoop is due to endogenous market dynamics governed by low-dimensional nonlinear behavior. The implication for food policy is that this inherently unstable market cannot be relied upon to systematically stabilize observed price volatility from random exogenous shocks. There may be scope for public interventions targeted to increasing the flexibility of organic fruit producers in responding to changing market conditions.

1. Introduction

Key international agencies and think tanks identify food-price volatility as a serious threat to food security (G20 2011; HLPE 2011; Kalkuhl et al. 2013). Policies broadly seek to reduce price volatility itself and/or buffer its negative impacts on consumers and producers through market-based strategies or public interventions (Galtier 2013; Gouel 2012). Market-based strategies are intended to reduce price volatility by improving market allocation of commodities spatially (through trade) and temporally (through storage), and to buffer negative impacts on producers through risk-hedging instruments in futures markets and, to a limited extent, on consumers through emergency aid during food crises. Public interventions are intended to reduce price volatility by controlling available market quantities with tools including price floors/ceilings, quantity restrictions, taxes and subsidies, and public buffer stocks, and to buffer negative impacts with transfer payments designed to protect producer incomes during periods of low prices and consumer's access to food levels during periods of high prices (Galtier 2013).

The consensus in the literature is that the effectiveness of public interventions depends on the agricultural price dynamics driving volatility. The dominant doctrine attributes volatility to exogenous random shocks that price adjustments dampen over time (Galtier 2013). In this framework, public interventions interfere with the market's 'natural correction process' (Gouel 2012). An alternative explanation is that price volatility persists in recurrent patterns due to the endogenous behavior of inherently unstable food markets responding to changes in supply and demand (Berg and Huffaker 2015; Chavas and Holt 1993; Galtier 2013). Agricultural markets do not provide a 'natural correction process' for price volatility.

Galtier (2013) concludes that distinguishing between endogenous and exogenous price volatility in particular agricultural markets "is still an open question, and the only certitude we have is that endogenous sources of instability can theoretically exist and affect all countries, with panics being far more probable…" (p. 74). In this paper, we propose a five-stage empirical diagnostic scheme—based on nonlinear dynamics techniques—to distinguish between endogenous and exogenous market dynamics in observed agricultural price series. Armed with this empirical evidence, policymakers can make an empirically-informed determination of whether laissez-faire or interventionist policies might be more effective in managing price volatility in particular cases.

* Corresponding author.
E-mail addresses: rhuffaker@ufl.edu (R. Huffaker), maurizio.canavari@unibo.it (M. Canavari).

http://dx.doi.org/10.1016/j.agsy.2016.09.019
0308-521X/

2. Past empirical approaches

Gouel (2012) surveys two main approaches that have been used to empirically distinguish between endogenous and exogenous food price volatility. A 'model-centric' approach tests for endogenous volatility by directly estimating theoretical market models. Models that fit the data well and/or conform to 'stylized facts' based on statistical properties of observed agricultural prices are deemed to provide empirically-validated explanations for endogenous volatility. An alternative 'data-centric' approach seeks to establish positive empirical evidence that observed volatility is generated endogenously by a particular type of nonlinear dynamics: low-dimensional chaos (Adrangi and Chatrath 2003; Chatrath et al. 2000).

The major problem with a model-centric approach is that a theoretical model cannot be validated by demonstrating a 'good fit' with observed data since other models with very different structures and representations of reality can be parameterized to also provide good fits (Hornberger and Spear 1981; Oreskes et al. 1994; Rykiel 1996). The commodity price literature provides an instructive case study. The empirical validity of the classic competitive storage model was challenged on the basis that it failed to account for the degree of serial correlation in observed commodity prices (Deaton and Laroque 1996). However, subsequent work demonstrated that a competitive storage model could be reformulated to improve empirical performance (Cafiero et al. 2011), and moreover that the measurement of price data used to estimate a given model could impact empirical performance (Guerra et al. 2015).

An additional problem with a model-centric approach is that the conformity of model output with 'stylized facts' based on probabilistic properties of observed prices does not resolve the price endogeneity question. The methodological standard set in the empirical nonlinear dynamics literature compares model dynamics with those empirically reconstructed from observed data based on shared topological properties (Kot et al., 1988).

An alternative data-centric approach—seeking positive evidence of endogenous chaotic dynamics in commodity price data—is also unreliable. The approach proceeds as follows: First, a price series is purged of linear dynamics and seasonal variation with a linear-autoregressive (ARCH/GARCH) model. Next, a phase-space attractor is reconstructed from the filtered price series using time-delay embedding (Takens 1980), and tested for topological features of chaos including 'self-similar geometry' (by measuring the correlation dimension), and 'sensitive dependence on initial conditions' (by measuring the Lyapunov exponent). The major drawback with relying on these measures to positively demonstrate chaotic dynamics in observed data is that they are based on asymptotic properties best met with vast amounts of high quality data provided by laboratory experiments designed specifically for investigating chaos (Schreiber 1999). The measures are unreliable when estimated from short and noisy real-world data (Chatrath et al. 2000; Schreiber 1999).

These topological measures perform reliably when the focus of empirical nonlinear analysis is relaxed from attempting to demonstrate the presence of deterministic chaos in observed data to gauging the degree to which endogenous nonlinear dynamics are present (Schreiber 1999; Schreiber and Schmitz 2000). Our proposed empirical nonlinear diagnostic scheme follows this path.

We apply nonlinear diagnostics to empirically reconstruct and characterize the dynamics of an organic fruit market from volatile organic apple, pear, orange and lemon prices (Euros per kilogram, €/kg) recorded weekly at the Milano Ipercoop over an eight-year interval (from 2003 to 2010, 421 weeks). The Ipercoop is the largest store format of the leading retail grocery chain in Italy (COOP)—a consumer cooperative with about 15% of the market share. Price data were provided by the Centro Servizi Ortofrutticoli (CSO), a cooperative company based in Ferrara (Italy), whose members are companies working in all phases of the fruit and vegetable supply chain. CSO collects weekly retail price data at selected stores in Italy and Europe. Consequently, the prices represent the evolution of a niche organic fruit market serving a limited number of consumers to a common retail market with widespread distribution (Canavari et al. 2002; Canavari and Olson 2007). We find strong empirical evidence that price volatility in the organic fruit market investigated is endogenously generated by nonlinear, low-dimensional and deterministic market dynamics.

How can we hope to reconstruct full market dynamics from observed price series? The answer is that the evolution of each price series encodes the historical interactions of driving market forces including consumer demand, fruit production, input costs, contracting practices, and so on; and nonlinear diagnostics recover this encoded information. The organic fruit price series used in this work illustrate well how market dynamics can be reconstructed from price data, and how reconstructed dynamics can guide subsequent formulation of realistic mechanistic market models using techniques such as dynamic systems modeling. The actual formulation of a mechanistic market model is beyond the scope of this paper.

3. An empirical nonlinear dynamics diagnostics scheme

We diagnose endogenous market dynamics as a source of observed price volatility as follows (Fig. 1): In Stage 1, we apply *Singular Spectrum Analysis* to separate each price series into endogenous structured volatility ('signal') and exogenous unstructured volatility ('noise') with signal processing techniques. In Stage 2, we test whether a detected signal is generated endogenously by nonlinear, low-dimensional and deterministic market dynamics with *Nonlinear Time Series Analysis* (Kantz and Schreiber 1997). In Stage 3, we conduct causal network analysis with *Convergent Cross Mapping* (Sugihara et al. 2012) to empirically test whether the dynamics of the observed organic fruit prices causally interact in the same market system. If so, in Stage 4, we simulate empirically-detected endogenous price volatility with a dynamic (phenomenological) market model composed of a system of ordinary differential equations (Baker et al. 1996), and use the model to investigate dynamic price interactions driving endogenous market dynamics. Finally, in Stage 5, we model exogenous noise with *Extreme Value Statistics* (Katz 2010)—a method currently used in the food security literature (Kalkuhl et al. 2013).

3.1. Signal processing

We apply *Singular Spectrum Analysis*—a 'data driven' signal processing method that accommodates highly anharmonic (potentially non-sinusoidal) oscillations in irregular time series data (Elsner and Tsonsis 2010)—to separate an observed price series into endogenous structured variation ('signal') and exogenous unstructured variation ('noise'). Signal incorporates trend and oscillatory components. Signal strength is measured as the fraction of variation explained in an observed price series from its mean when the price series is converted to an anomaly from its mean, and the *Toeplitz* method of *SSA* is applied (Ghil et al. 2002; Golyandina et al. 2001). Signal strength provides preliminary empirical evidence for the relative contribution of endogenous to exogenous volatility. Positive (negative) noise levels occur at times when an observed price series is greater (less) than the corresponding signal.

Singular Spectrum Analysis can be applied to fill in intermittent missing values in observed data by using dynamic structure detected from the full range of reported observations to calculate replacements for missing values. Consequently, it processes more information than conventional moving average approaches limited to observations immediately surrounding the missing values (Golyandina et al. 2001).

3.2. Nonlinear time series analysis

We apply *Nonlinear Time Series Analysis* (*NLTS*) (Kantz and Schreiber 1997) to test whether structured volatility separated in signal

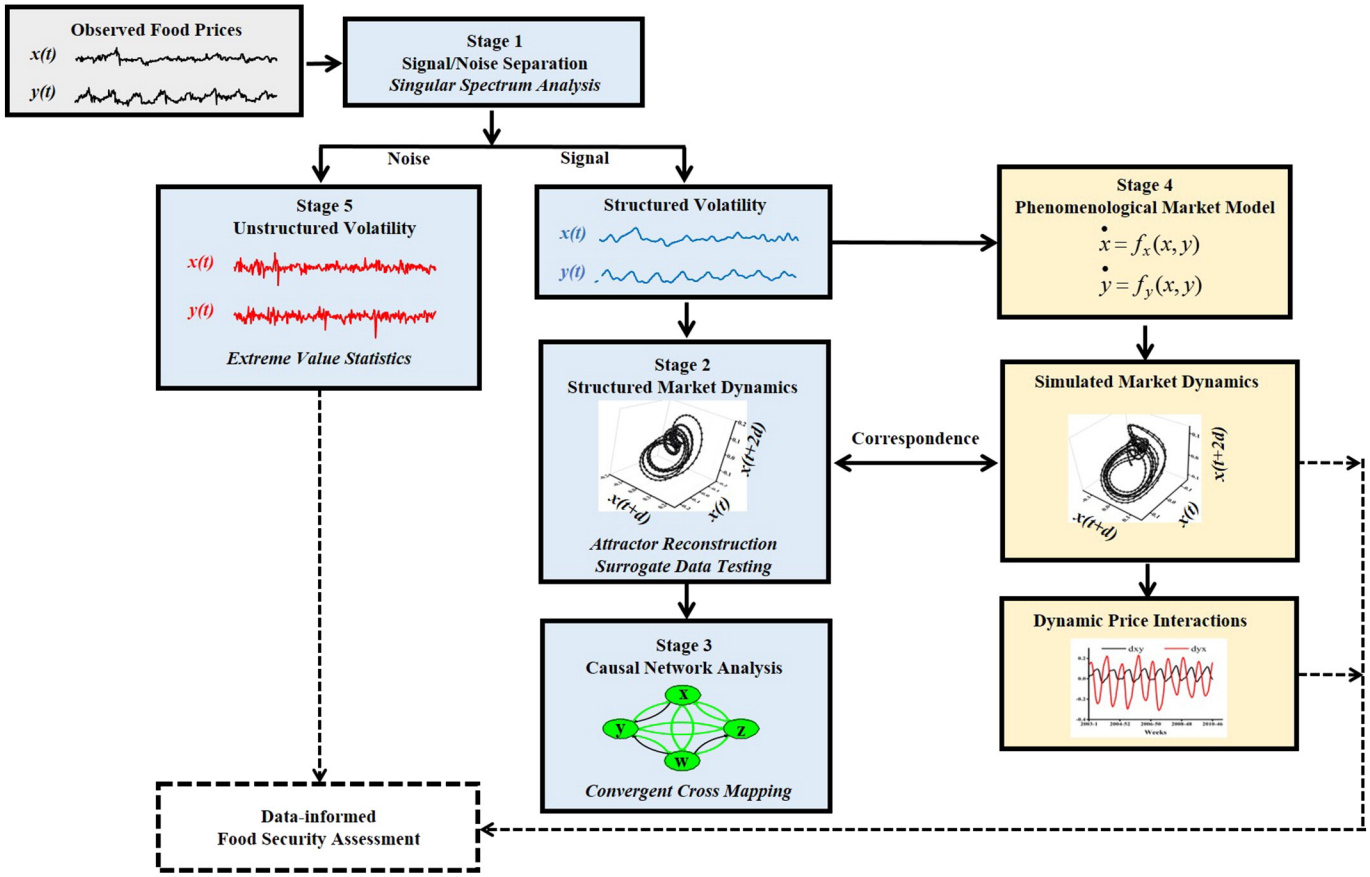

Fig. 1. Empirical scheme for distinguishing between endogenous and exogenous price volatility. In Stage 1, *Singular Spectrum Analysis* separates observed price series into endogenous structured volatility (signal) and exogenous unstructured volatility (noise). In Stage 2, price signals are tested for low-dimensional, nonlinear endogenous market dynamics with *Phase Space Reconstruction* and *Surrogate Data Testing*. In Stage 3, *Convergent Cross Mapping* identifies causal network interactions among detected price signals. In Stage 4, detected endogenous volatility is simulated with a phenomenological market model to understand price interactions driving endogenous volatility. In Stage 5, exogenous volatility is analyzed with *Extreme Value Statistics*. Policymakers can use diagnosed information to make a data-informed choice of whether laissez-faire or interventionist policies will be most effective in reducing price volatility.

processing is generated endogenously by nonlinear, low-dimensional and deterministic market dynamics. Similar to other time series methods, *NLTS* demands stationary data which is promoted by extracting the trend from each price signal.

The centerpiece of *NLTS* is *Phase Space Reconstruction*—the reconstruction of real-world system dynamics from a single observed time series. In general, points in phase space represent the 'state' of a dynamic system given by the level of system variables in given time periods. Each point evolves along a unique trajectory governed by a system of (usually) first-order differential equations. If the dynamic system is 'dissipative', system variables co-evolve from given initial conditions toward a geometric structure ('attractor') with "noticeable regularity" ((Brown 1996), p. 55). Attractors include stable fixed points, stable limit cycles, and chaotic structures upon which solution trajectories oscillate irregularly (Glendinning 1994; Strogatz 1994).

We illustrate *Phase Space Reconstruction* using the following linear-cobweb market model with two interacting prices $p_x(t)$ and$p_y(t)$:

$$\begin{aligned} p_x(t+1) &= 0.9p_x(t) + 0.3p_y(t) + 100 \\ p_y(t+1) &= -0.3p_x(t) + 0.9p_y(t) + 100 \end{aligned} \tag{1}$$

The prices solving this dynamic system—plotted as time series in Fig. 2a—oscillate toward a steady-state market equilibrium. The market dynamic—pictured in phase space by plotting one price against the

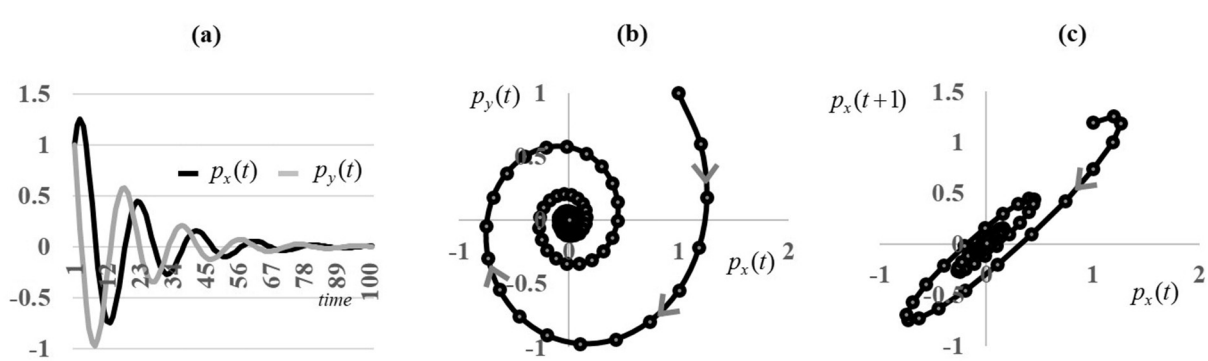

Fig. 2. Linear cobweb price dynamics: (a) Time series plots, (b) Phase-space market attractor, (c) *Phase Space Reconstruction* of the market attractor using a single price.

Please cite this article as: Huffaker, R., et al., Distinguishing between endogenous and exogenous price volatility in food security assessment: An empirical nonlinear dynamics appr..., Agricultural Systems (2016), http://dx.doi.org/10.1016/j.agsy.2016.09.019

other at each point time in Fig. 2b—has the two prices co-evolving along the familiar cobweb trajectory toward market equilibrium. The systematic cobweb cycle is an example of a phase-space attractor. Depending on system parameters, the linear market system can also produce a center-point equilibrium around which prices co-evolve periodically. The market model must be reformulated with nonlinear feedback between the two prices to produce a more complex attractor, for example, one upon which variables cycle aperiodically (Dieci and Westerhoff 2009; Hommes 1991; Jensen and Urban 1984; Zachilas and Gkana 2011).

A 'shadow' version of the cobweb market attractor can be reconstructed by plotting one of the prices, e.g., $p_x(t)$, against its level one period later, $p_x(t+1)$ (Fig. 2c). Two-dimensional phase space in original price coordinates is reproduced by a single price and one of its forward-delayed copies. This is the *Time Delay Embedding* approach to *Phase Space Reconstruction* that reconstructs system dynamics (i.e., the cobweb attractor) from a single time-series variable. Takens (1980) derived sufficient conditions guaranteeing time-delay embedding to be a 1:1 mapping of dynamics from original-system to time-delay coordinates (Takens 1980). This means that the reconstructed shadow market attractor preserves essential dynamic properties of the original attractor.

While the above example demonstrates how system dynamics can be reconstructed from one system variable, it does not demonstrate the full potential of *Phase Space Reconstruction* since the linear-system cobweb dynamic is already obvious in the time series plots. The utility of Phase Space Reconstruction is to reconstruct nonlinear system dynamics concealed in volatile and random-appearing observed data.

In general empirical application, an observed price signal *p(t)* is segmented into a sequence of delay coordinate vectors: *p(t)*, *p(t-d)*, *p(t-2d)*,…, *p(t-(m-1)d)*, where *d* is the 'time delay' and *m* is the number of delayed coordinate vectors (the 'embedding dimension'). The sequence of delay coordinate vectors is collected as columns in an 'embedded data' matrix, and the reconstructed phase space is a scatterplot of the multidimensional points constituting the rows of this matrix:

$$P,(t) = \{p(t), p(t-d), p(t-2d), p(t-(m-1)d\}, t = 1, ..., T \tag{2}$$

where T is the terminal time period. The embedding dimension is conventionally selected with the 'false nearest neighbors' test (Williams 1997). This test measures the percentage of close neighboring points on an attractor in a given embedding dimension that grow apart in the next highest dimension (i.e., 'false neighbors'). The embedding dimension selected for the shadow attractor is that for which the percentage of false neighbors falls below a given tolerance level. The embedding delay is conventionally selected as the first minimum of the 'mutual information function'—a probabilistic measure of the extent to which a variable is related to its delayed value (Williams 1997). This selection is designed to introduce statistical independence between successive delayed values. Too short a delay does not give system dynamics an adequate opportunity to evolve, while too long a delay causes reconstruction to skip over important dynamic structure.

The next step in empirically diagnosing endogenous market dynamics is to rule out the possibility that an empirical attractor's noticeable geometric regularity is mimicked by a linear stochastic process (Schreiber and Schmitz 2000; Small and Tse 2002, 2003; Theiler et al. 1992). First, each de-trended price signal is used to randomly generate a set of surrogate price vectors. For example, a set of N surrogates generated from an observed price signal, $P_i(t)$, is:

$$P_i(t) = \begin{bmatrix} P_i(0) \\ P_i(1) \\ \cdot \\ \cdot \\ \cdot \\ P_i(T) \end{bmatrix} \Rightarrow \left\{ P_i^{S_1}(t) = \begin{bmatrix} P_i^{S_1}(0) \\ P_i^{S_1}(1) \\ \cdot \\ \cdot \\ \cdot \\ P_i^{S_1}(T) \end{bmatrix}, P_i^{S_2}(t) = \begin{bmatrix} P_i^{S_2}(0) \\ P_i^{S_2}(1) \\ \cdot \\ \cdot \\ \cdot \\ P_i^{S_2}(T) \end{bmatrix}, ..., P_i^{S_N}(t) = \begin{bmatrix} P_i^{S_N}(0) \\ P_i^{S_N}(1) \\ \cdot \\ \cdot \\ \cdot \\ P_i^{S_N}(T) \end{bmatrix} \right\} \tag{3}$$

where $P_i^{S_1}(t), P_i^{S_2}(t), \ldots, P_i^{S_N}(t)$ are surrogate price vectors, and T is the length of an observed price series. The surrogates are formulated to destroy intertemporal patterns in the signal while preserving various statistical properties.

Amplitude Adjusted Fourier Transform (*AAFT*) surrogates are "static monotonic nonlinear transformations of linear filtered noise" designed to preserve a signal's probability distribution and power spectrum [(Small and Tse 2003), p. 664]. Shortcomings of the *AAFT* algorithm—the most widely used—led to recommendations that a more general algorithm be developed to test the null hypothesis that real-world dynamics are characterized by a noisy limit cycle (Theiler et al. 1992). In response, *Pseudo Phase Space* (*PPS*) surrogates were designed to replace a signal's dynamic structure with linearly-filtered noise whose dynamics are characterized by a randomly-shifting limit-cycle attractor (Small and Tse 2002). Consequently, *PPS* surrogates are used to test the null hypothesis that nonrepeating cycling detected in an empirically-reconstructed attractor is most likely due to a randomly-shifting limit cycle characteristic of stochastic linear dynamics (Nicholson and Stephensen 2015). We follow (Kugiumtzis 1999) in first testing the null hypothesis of linear stochastic dynamics with the *AAFT* algorithm, and then re-testing with the more general *PPS* algorithm.

Next, phase space is reconstructed for each surrogate vector, and selected *discriminating statistics* measuring various attractor characteristics are estimated. Conventional discriminating measures for detecting 'hallmarks' of deterministic structure in an attractor include the 'correlation dimension' (measuring the extent to which points on a reconstructed attractor are spatially organized), and the 'Lyapunov exponent' (measuring sensitivity to initial conditions and resultant spreading of state-space trajectories over time) (Kantz and Schreiber 1997; Schreiber 1999). Although these two discriminating statistics must be used with great care in empirical work because of difficulties in computing reliable estimates from finite noisy records, they can be reliably used to distinguish between deterministic and random structure in surrogate data tests (Schreiber 1999).

Another conventional discriminating measure is an attractor's short-term predictive skill (Small and Tse 2002; Theiler et al. 1992). Points on an attractor are divided into forecasting and validation bases. Initially, the nearest neighboring points to the final point in the forecast base are identified, advanced one time period, and averaged to forecast the first point in the validation base. At each step, the forecasting base is augmented by a point in the validation base until all points (excepting the final point) are validated (Kantz and Schreiber 1997; Kaplan and Glass 1995; Sprott 2003). Nash-Sutcliffe Model Efficiency (*NSE*) is a conventional discriminating measure of the goodness-of-fit between in-sample predictions and the validation base (Ritter and Muñoz-Carpena 2013):

$$NSE = 1 - \frac{\sum_{i=1}^{N} (p_i - p_{Fi})^2}{\sum_{i=1}^{N} (p_i - \overline{p})^2} \tag{4}$$

where N denotes periods in the validation base, p and p_F are the price signal and its forecasted value, respectively, and $\overline{p}$ is the price signal averaged over the validation base. A value $NSE = 1$ represents a perfect fit, and $NSE > 0.65$ is often proposed as a model quality threshold (Ritter and Muñoz-Carpena 2013).

We follow conventional practice in testing the null hypothesis of linear-stochastic dynamics with nonparametric rank-order statistics (Schreiber and Schmitz 2000; Theiler et al. 1992). There are $S = (2k/\alpha) - 1$ surrogate data vectors generated for a two-tailed test, where α sets the probability of false rejection, $(1-\alpha) \times 100$ is the level of significance, and k determines the number of generated surrogates with larger k values providing more sensitive tests. Linear stochastic dynamics are rejected if a discriminating statistic taken from the empirical-reconstructed attractor is among the k smallest or k largest values in the ensemble of statistics taken from the surrogate attractors. There are $S = (k/\alpha) - 1$ surrogates generated for a single tailed test, and linear stochastic dynamics are rejected if a discriminating statistic taken from the

empirical-reconstructed attractor is among the k smallest (for a lower-tailed test) or k largest (for an upper-tailed test). We conduct a two-tailed test for correlation dimension and Lyapunov exponent, and a single-tailed test for predictive skill to reject the null hypothesis only if the empirically-reconstructed attractor predicts with more skill that its surrogate counterparts.

3.3. Causal network analysis

Sugihara et al. (2012) recently developed *Convergent Cross Mapping* (*CCM*) to detect causal networks in low-dimensional, nonlinear and deterministic dynamic systems. If prices X and Y interact in the same market, then an attractor reconstructed with either delayed X-coordinates (A_X) or delayed Y-coordinates (A_Y) both map 1–1 to the original market attractor (A), and consequently map 1–1 to each other.

To test whether a 1–1 mapping exists between A_Y and A_X, a reference time period is selected, and the corresponding points on the two attractors are identified. Next, the time indices associated with the nearest neighbors to the reference point on A_Y (for example) are identified. These time indices also yield nearest neighbors to the reference point on A_X only if there is a 1–1 mapping with A_Y. Such 'cross mapping' can be used to predict states of X from the historic record for Y, and vice-versa. Skillful cross predictions indicate that X and Y are causally related. A measure of the strength of causal interaction is that cross-mapped predictions of X using A_Y converge toward the observed value as the portion of the historic record for Y used to reconstruct A_Y increases in length. The goodness-of-fit between the two can be measured with the *Pearson Correlation Coefficient*. Stronger causal interaction is indicated as both statistics converge closer to one (Sugihara et al. 2012).

3.4. Phenomenological market modeling

Convergent Cross Mapping tests whether prices interact in the same dynamic market system, but does not characterize the nature of interactions, for example, whether an increase in one price decreases the growth rate of others. We formulate a phenomenological (data-driven) model to investigate dynamic price interactions driving detected real-world endogenous market volatility (Baker et al. 1996; Wei-Dong et al. 2003). The model is composed of a system of ordinary differential equations (*ODEs*), each *ODE* linking the growth rate of a price signal to a polynomial function in all of the signals:

$$\begin{aligned} \dot{P}_1 &= \dot{P}_1(P_1(t), P_2(t), \ldots, P_n(t)) \\ \dot{P}_2 &= \dot{P}_2(P_1(t), P_2(t), \ldots, P_n(t)) \\ &\ldots \\ \dot{P}_n &= \dot{P}_n(P_1(t), P_2(t), \ldots, P_n(t)) \end{aligned} \tag{5}$$

Growth rates are approximated by taking 4th order centered finite differences of each signal. The order of polynomials is selected so that the market model faithfully reproduces the empirical attractor, and simulated price signals reproduce the spectral properties of the observed signals. Since the model is linear in parameters, it can be fit with *Ordinary Least Squares* (*OLS*) or *Partial Least Squares Regression* techniques if needed to correct for possible collinearity among polynomial regressors (Mevik and Wehrens 2007).

Following the ecosystems literature (Hastings 1978), we classify pairwise interactions between two price signals by the marginal impact that an incremental increase in price i has on the growth rate of price j and vice versa; that is, by the signs of time-varying cross partial derivatives taken from phenomenological model (5): $\frac{\partial \dot{P}_j}{\partial P_i}(t)$, $\frac{\partial \dot{P}_i}{\partial P_j}(t)$. Positive cross derivatives signify that $P_i(t)$ and $P_j(t)$ engage in a 'mutually beneficial' interaction that generates marginal increases in both. Negative cross derivatives indicate a 'competitive' or mutually-detrimental interaction resulting in marginal reductions in both price signals. Finally, cross derivatives of opposite sign indicate a 'predator-prey' interaction in which, for example, the *jth* price signal (enjoying positive marginal growth) 'preys' on the *ith* price signal (suffering negative marginal growth).

3.5. Extreme Value Statistics

We apply *Extreme Value Statistics* (Katz 2010) to model exogenous volatility contained in unstructured noise separated from each observed price series. *Extreme Value Statistics* calculate the likelihood of extreme price volatility exceeding a selected threshold value within some time interval. A conventional way to select a threshold value is the noise level at which the *mean-residual-life* plot becomes linear with increasing thresholds (Gilleland 2015). Exceedances follow a *Generalized Pareto* (*GP*) distribution whose quantiles produce a 'return level plot' that estimates the 'return' time expected before extreme volatility of a particular magnitude ('return level') is realized.

3.6. Computational packages

The following **R** packages are available to run the above procedures. *Singular Spectrum Analysis*: *RSSA* (Golyandina and Korobeynikov 2014); *Phase Space Reconstruction* and *Surrogate Data Analysis*: 'tseriesChaos' (Di Narzo and Di Narzo 2013), 'nonlinearTseries' (Garcia 2015), and 'fractal' (Constantine and Percival 2014); *Convergent Cross Mapping*: 'multispatialCCM' (Clark 2014); Network diagrams: 'igraph' (Csardi and Nepusz 2006); *Ordinary Least Squares Regression* used in *Phenomenological Modeling*: 'stats'; ODE solver used in *Phenomenological Modeling*: 'deSolve' (Soetaert et al. 2015); and *Extreme Value Statistics*: 'extRemes' (Gilleland and Katz 2011).

4. Results

Our results provide compelling empirical evidence of endogenous price volatility generated by a nonlinear, low-dimensional and deterministic market dynamic in the observed Italian organic fruit market.

In Stage 1, we converted each price series to an anomaly from its mean, and initially applied *Singular Spectrum Analysis* to fill in intermittent missing values in the recorded apple, pear, orange and lemon prices. Next, price anomalies were decomposed into signal (containing trend and dominant annual and semiannual cycles) and unstructured noise. Price signals account for the majority of variation in each price series from its mean (Table 1). The plots of observed price anomalies (green lines), price signals (black lines), isolated trends (blue lines), and unstructured noise (red lines) for each commodity are displayed in Fig. 3. Annual oscillations for apple-price (3a) and pear-price (3b) signals increase from about October until June, and then decline for two to three months. The annual oscillation for the orange-price signal (3c) increases from about January to October, and then declines for two to three months. The annual oscillation for the lemon-price signal (3d) increases from about April to September and declines from October to March.

In Stage 2, we successfully reconstructed empirical market attractors with 'noticeable regularity' from the (detrended) price signals (Fig. 4a–d). The attractors exhibit non-repeating aperiodic oscillations characterized by the dominant annual and weaker semi-annual cycle lengths

Table 1
Signal processing: percent variance in observed data explained.[a]

	Signal	Trend	53 w	26.5 w
Apple prices	55%	29%	17%	9%
Pear prices	72%	15%	53%	4%
Orange prices	61%	12%	49%	–
Lemon prices	61%	47%	14%	–

[a] Observed time series converted to anomalies from the mean (w = week).

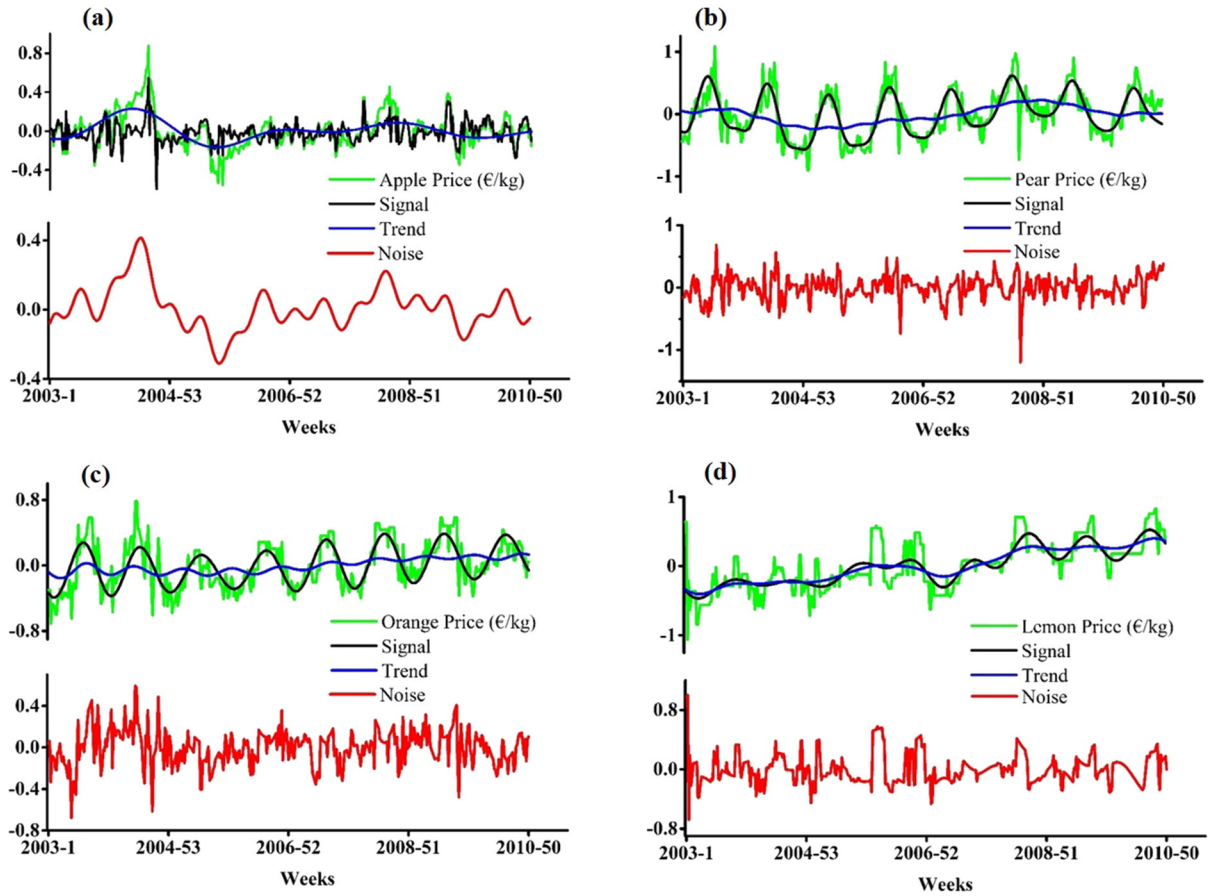

Fig. 3. Signal/Noise separation. *Singular Spectrum Analysis* separates each price series (grey line) into signal (black line) and noise (red line). The time (horizontal) axis shows year and week, e.g., 2003-1 denotes the first week of 2003. Price signals incorporate endogenous variation. Price signals are strong—ranging from 55% to 72% of total variance in observed price series—and are composed of trend (isolated by blue line) and dominant annual and semiannual cycles. Noise is residual exogenous variation. Positive (negative) noise levels occur at times when an observed price series is greater (less) than the corresponding signal. (For interpretation of the references to color in this figure legend, the reader is referred to the web version of this article.)

uncovered in signal processing. Surrogate data tests soundly rejected the null hypothesis that the attractors' 'noticeable regularity' is due to a mimicking linear stochastic market dynamic consistent with exogenous price volatility. We set the significance level at 95% resulting in 99 surrogates generated for each of the two-tailed tests on correlation dimension and Lypunov exponent, and 49 surrogates for the single-tailed test on predictive skill. When using *AAFT* surrogates, the null hypothesis was rejected for the attractors reconstructed from pear and orange prices for all three discriminating measures, and accepted for the attractors reconstructed from apple and lemon prices only for one of the measures (Table 2). These results hold for the *PPS* surrogates (Table 3).

In Stage 3, *Convergent Cross Mapping* results provide strong empirical evidence that signals for apple prices, pear prices, orange prices, and lemon prices are causally interrelated (Fig. 5). The attractors reconstructed from each price signal skillfully cross-predict the other signals at saturated correlation coefficients above $\rho \approx 0.8$ (Fig. 5a–d). These causal interactions are summarized in a network diagram where arrows indicate directions of causality, and color denotes strength of causality (Fig. 5e).

In Stage 4, we found that second-order polynomial price interactions provided a good fit for the *ODE* associated with each price signal:

$$\dot{P}_i \approx \alpha_{i0} + \alpha_{i1}P_{lemon} + \alpha_{i2}P_{orange} + a_{i3}P_{orange}P_{lemon} + \alpha_{i4}P_{pear} + \alpha_{i5}P_{pear}P_{lemon} + \alpha_{i6}P_{pear}P_{orange} + \alpha_{i7}P_{pear}P_{orange}P_{lemon} + \alpha_{i8}P_{apple} + a_{i9}P_{apple}P_{lemon} + a_{i10}P_{apple}P_{orange} + \alpha_{i11}P_{apple}P_{orange}P_{lemon} + a_{i12}P_{apple}P_{pear} + a_{i13}P_{apple}P_{pear}P_{lemon} + a_{i14}P_{apple}P_{pear}P_{orange} + a_{i15}P_{apple}P_{pear}P_{orange}P_{lemon} \quad (6)$$

where i indexes the apple signal, pear signal, orange signal, and lemon signal; and estimated *OLS* coefficients are found in Table 4. *Cumulative Distribution Functions* (*CDFs*) and 95% confidence intervals for *NSE* were generated by block-bootstrapping of the observed and predicted values for each equation (Ritter and Muñoz-Carpena 2013). These were used to strongly reject the null hypothesis that *NSE* falls below the 0.65 minimum model quality threshold with probability values $p = 0$ (Table 4) (Ritter and Muñoz-Carpena 2013). Another indication of good fit is that the phenomenological model successfully simulated empirically-detected endogenous price dynamics. The simulated attractor reconstructed from model solutions for the apple-price signal (Fig. 4e) bears striking resemblance to the empirical attractor reconstructed from observed apple-price anomalies (Fig. 4a), and exhibits similar discriminating statistics. Both have an embedding delay of 9 weeks. The simulated attractor has a correlation dimension of 2.04, a Lypunov exponent of 0.08, and predictive skill given by $NSE = 0.99$. The values for the empirical attractor are 2.45, 0.05, and NSE = 0.97, respectively.

We applied the phenomenological market model to find that empirically-detected endogenous price dynamics are driven by remarkably systematic pairwise interactions among the signals for apple prices, pear prices, orange prices, and lemon prices. Consider, for example, pairwise interactions between the apple-price and pear-price signals (Fig. 6a). The plots of both cross derivatives alternate between positive and negative through time. Both are positive from January through February each year indicating that an incremental increase in one price has a positive impact on the growth rate of the other—a mutually beneficial or 'symbiotic' relationship. During the remaining months of each year, pear prices have a positive impact on the growth of apple prices,

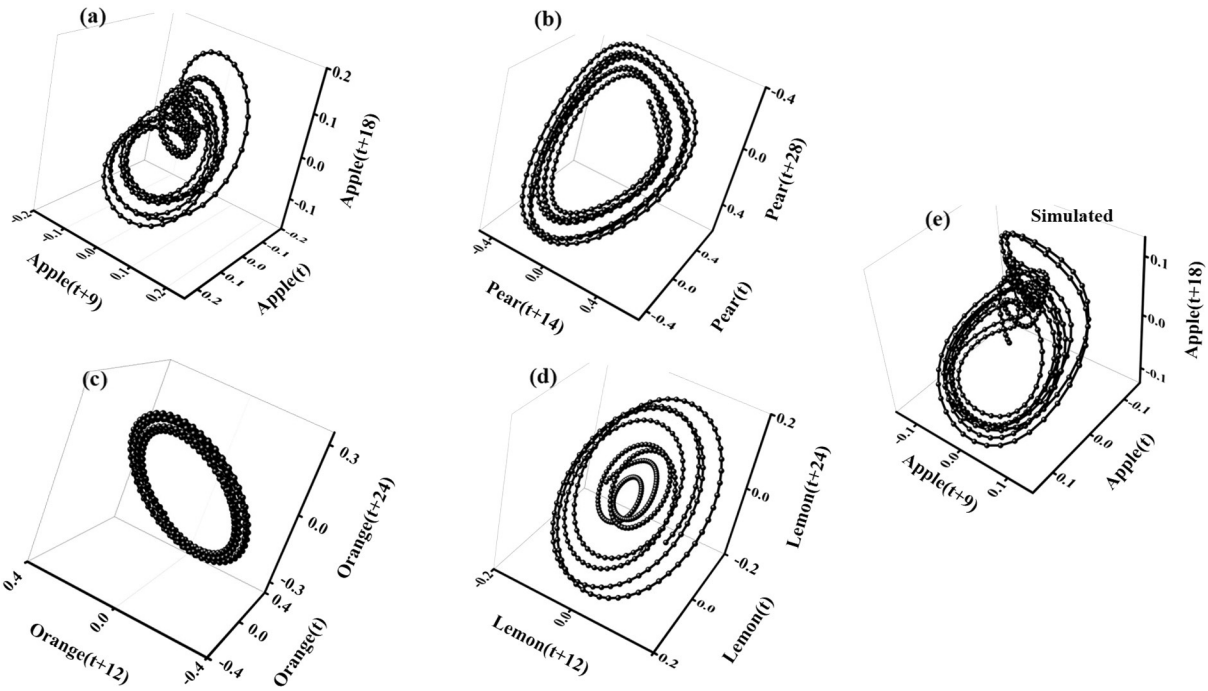

Fig. 4. The empirical attractors constructed from the price signals for organic (a) apples, (b) pears, (c) oranges, and (d) lemons. The empirical attractors demonstrate 'noticeable regularity' which offers preliminary evidence that observed volatility in the corresponding price series is driven by endogenous low-dimensional nonlinear market dynamics. Fig. 4e shows that the attractor reconstructed from the apple-price signal simulated by the phenomenological market model bears striking resemblance to the empirical attractor (Fig. 4a), and thus that the phenomenological model corresponds well to diagnosed real-world market dynamics.

while apple prices have negative impact on the growth of pear prices—apple prices 'prey' on pear prices. In other pairwise interactions, orange prices 'prey' on apple prices from approximately October to April each year, while the cross derivatives turn negative during the remaining months indicating that the relationship turns 'competitive' (Fig. 6b). Apple prices 'prey' on lemon prices from about May to October each year, and the relationship turns 'symbiotic' over the remaining months (Fig. 6c). Orange prices 'prey' on pear prices all year (Fig. 6d). Pear prices 'prey' on lemon prices from approximately November through February and May through August, and the relationship turns competitive from March through April and September through October (Fig. 6e). Finally, orange and lemon prices are symbiotic in December and January and competitive the rest of the year (Fig. 6f). The above pairwise dynamic price interactions are summarized in Table 5.

In Stage 5, we applied *Extreme Value Statistics* to probabilistically model the exogenous volatility (noise) separated from each price series, and compute return-level plots that estimate expected 'return' times before extreme positive and negative exogenous volatility levels exceed selected thresholds (Fig. 7). The thresholds selected for each price signal, the total number of exceedances over the length of the price series, and the weekly exceedance rate are reported in Table 6. For example, noise separated from observed apple-price anomalies exhibits extreme positive discrepancies (in which observed price anomalies are greater than the signal) exceeding a threshold of 0.05 €/kg a total of 115

Table 2
AAFT surrogate data results using rank-order statistics.[a]

Apple prices	Signal	Surrogate (low)	Surrogate (high)	H_0
Correlation dimension	2.45	2.46	3.52	Reject
Lyapunov exponent	0.05	0.07	0.39	Reject
Predictive skill	0.97	0.92	0.97	Accept
Pear prices				
Correlation dimension	1.46	1.53	1.98	Reject
Lyapunov exponent	0.09	0.13	0.55	Reject
Predictive skill	0.99	0.92	0.98	Reject
Orange prices				
Correlation dimension	1.26	1.39	1.68	Reject
Lyapunov exponent	0.12	0.11	0.58	Reject
Predictive skill	1.00	0.95	0.99	Reject
Lemon prices				
Correlation dimension	2.79	1.8	2.92	Accept
Lyapunov exponent	0.04	0.07	0.39	Reject
Predictive skill	0.99	0.93	0.98	Reject

[a] *AAFT* surrogates are used to test the null hypothesis that nonrepeating cycling characterizing the empirically-reconstructed attractors is generated by linear stochastic dynamics. The significance level is set at 95% resulting in 99 surrogates for correlation dimension and Lyapunov exponent (two-sided tests), and 49 surrogates for predictive skill (one-sided test).

Table 3
PPS surrogate data results using rank-order statistics.[a]

Apple prices	Signal	Surrogate (low)	Surrogate (high)	H_0
Correlation dimension	2.45	2.29	3.32	Accept
Lyapunov exponent	0.05	0.86	1.65	Reject
Predictive skill	0.97	−0.15	0.32	Reject
Pear prices				
Correlation dimension	1.46	2.01	3.93	Reject
Lyapunov exponent	0.09	0.7	1.48	Reject
Predictive skill	0.99	0.16	0.68	Reject
Orange prices				
Correlation dimension	1.26	2.31	4.03	Reject
Lyapunov exponent	0.12	0.76	1.5	Reject
Predictive skill	1	0.27	0.68	Reject
Lemon prices				
Correlation dimension	2.79	2.40	3.37	Accept
Lyapunov exponent	0.04	0.82	1.57	Reject
Predictive skill	0.99	−0.09	0.38	Reject

[a] PPS surrogates are used to test the null hypothesis that nonrepeating cycling detected in the empirically-reconstructed attractors is most likely due to a randomly-shifting limit cycle characteristic of stochastic linear dynamics. The significance level is set at 95% resulting in 99 surrogates for correlation dimension and Lyapunov exponent (two-sided tests), and 49 surrogates for predictive skill (one-sided test).

Please cite this article as: Huffaker, R., et al., Distinguishing between endogenous and exogenous price volatility in food security assessment: An empirical nonlinear dynamics appr..., Agricultural Systems (2016), http://dx.doi.org/10.1016/j.agsy.2016.09.019

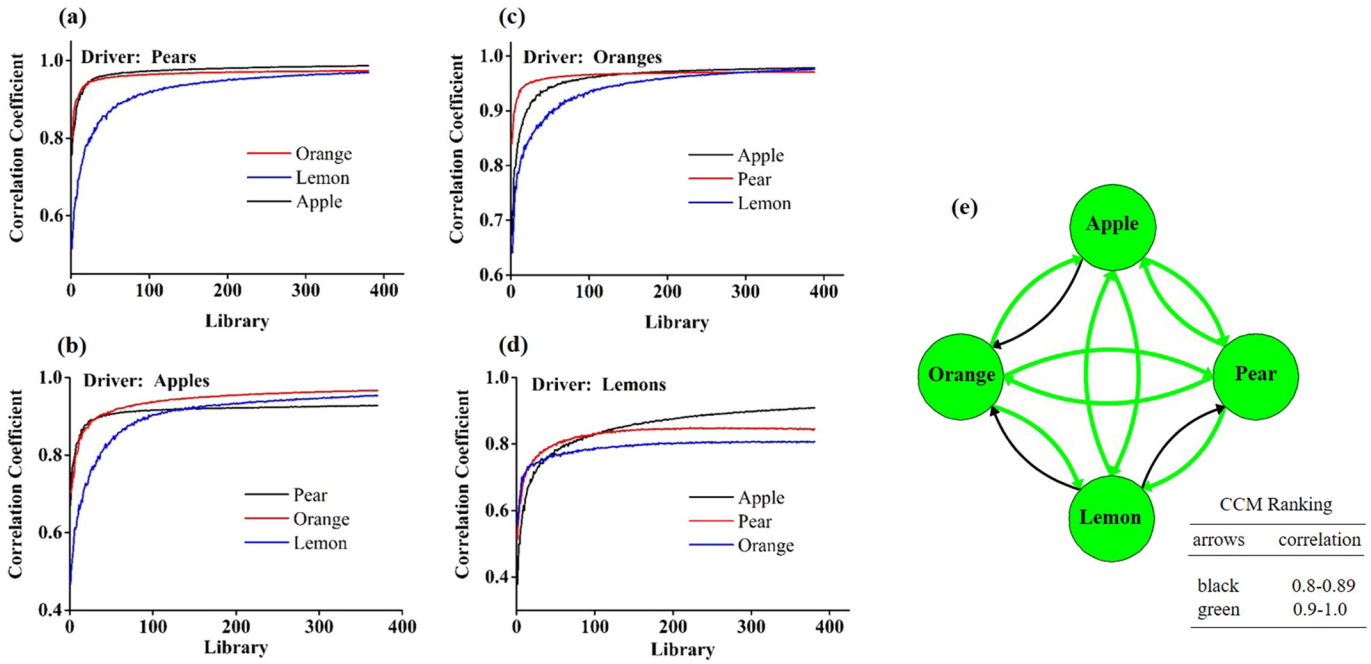

Fig. 5. Causal network analysis. *Convergent Cross Mapping* provides strong empirical evidence that the attractors reconstructed from observed price series represent the dynamics of the same real-world market system, and thus that the corresponding prices causally interact. The plots (a–d) show that the attractors reconstructed from each price series skillfully cross predict the other price signals. An attractor skillfully cross predicts another variable when the Pearson correlation coefficient (vertical axes) converges to a high value as the number of points on the attractor used to cross predict increases (horizontal axes). The cross-predictions in 4a–d are summarized in network diagram (4e) where arrows indicate directions of causality, and color denotes strength of causality. Green arrows denote a high-level saturated correlation coefficient interval (0.9, 1), and black arrows an intermediate interval (0.8, 0.89). (For interpretation of the references to color in this figure legend, the reader is referred to the web version of this article.)

times over the 421-week sample—about 27% of the time. Extreme negative discrepancies (in which observed price anomalies are less than the signal) exceed a threshold of 0.08 €/kg in absolute value a total of 126 times—about 30% of the time. The return-level plot for positive exceedances (Fig. 7, upper left corner) shows that noise separated from apple-price anomalies is expected to exceed larger discrepancies of 0.095 €/kg about every 5 weeks, 0.31 €/kg every 26 weeks, and 0.39 €/kg every 53 weeks (Table 7). Extreme negative discrepancies (Fig. 7, lower left corner) exceed the (absolute value) threshold of 0.12 €/kg about 5 weeks, 0.17 €/kg every 26 weeks, and 0.22 €/kg every 53 weeks (Table 7).

Table 4
OLS estimated coefficients to phenomenological market model.

Monomials[a]	*x.ODE*	*y.ODE*	*z.ODE*	*w.ODE*
Constant	−0.0075***[b]	0.0156***	0.0063***	0.0008
w	−0.0008	−0.0345**	−0.1428***	−0.0943***
z	−0.0512***	−0.2469***	−0.0602***	0.0575***
zw	−0.1162*	−0.1006	−0.0033	−0.0658
y	0.0486***	0.1492***	0.0712***	−0.0064***
yw	−0.0242	0.0628	0.0500	0.0184
yz	0.1837***	−0.2355***	−0.0216	0.0457***
yzw	−0.1258	2.1798***	2.2323***	1.1748***
x	−0.0457***	0.0466	0.1105***	0.0757***
xw	0.0511	1.0437***	0.4574**	0.3057**
xz	−0.2749***	−1.4078***	−0.6975***	−0.5286***
xzw	1.0441	−2.3595	−2.5276***	−1.0192*
xy	0.2654***	0.4980***	0.0555	0.1931***
xyw	1.5945**	4.5198***	2.7684***	2.8643***
xyz	−1.2060***	−1.3417***	−0.3897	−0.9513***
xyzw	1.7467	−2.5013	−7.4221***	−5.3977***
NSE[c]	0.85	0.89	0.91	0.8
	[0.83, 0.87]	[0.87, 0.91]	[0.9, 0.92]	[0.78, 0.83]
p-Value[d]	0.00	0.00	0.00	0.00

[a]Variables are apple prices (x), pear prices (y), orange prices (z), and lemon prices (w). The price series are converted to anomalies from the mean. The notation '*.ODE' represents the fitted ordinary differential equation for the variable; [b]t values; [c]95% confidence interval in brackets; [d]p(NSE ≤ 0.65); significance codes: ***lower than α = 0.01, **lower than α = 0.05, *lower than α = 0.10.

5. Discussion

Empirical diagnostics provide striking evidence that observed volatility in organic apple, pear and orange prices in this Italian market is due to inherent market instability governed by low-dimensional nonlinear dynamics. Long-term market dynamics evolve along a three-dimensional attractor empirically constructed from detected price signals. Surrogate data tests soundly reject the null hypothesis that the noticeable geometric regularity in these attractors is the figment of a mimicking linear stochastic process. The empirically-diagnosed market dynamics are successfully reproduced in a parsimonious four-dimensional deterministic system of *ODEs* composed of second-order polynomials. A market attractor reconstructed from simulated apple prices exhibits the same behavior as its empirically-reconstructed counterpart. The model provided a framework for characterizing systematic price interactions driving endogenous volatility. This showcases the potential for parsimonious deterministic models to capture and characterize the behavior of complex market systems. Saltelli and Funtowitz (2014) propose that parsimony be included in post-modeling auditing of theoretical models used in public policy because "simple or parsimonious model representations are better than more 'sophisticated' or complex models, when they are being used for policy impact assessments" (p. 84).

The diagnosed information can inform further effort to formulate a mechanistic fruit market model in the study area with techniques such as dynamic systems modeling. First, signal processing identifies the oscillatory periods in observed price series that should be matched by their simulated counterparts. Second, phase space reconstruction provides a geometric picture of long-term market dynamics that the solution to a mechanistic model should simulate to correspond to reality. Simulated market dynamics that undergo a cobweb adjustment to equilibrium, or that oscillate periodically, do not correspond to the aperiodic

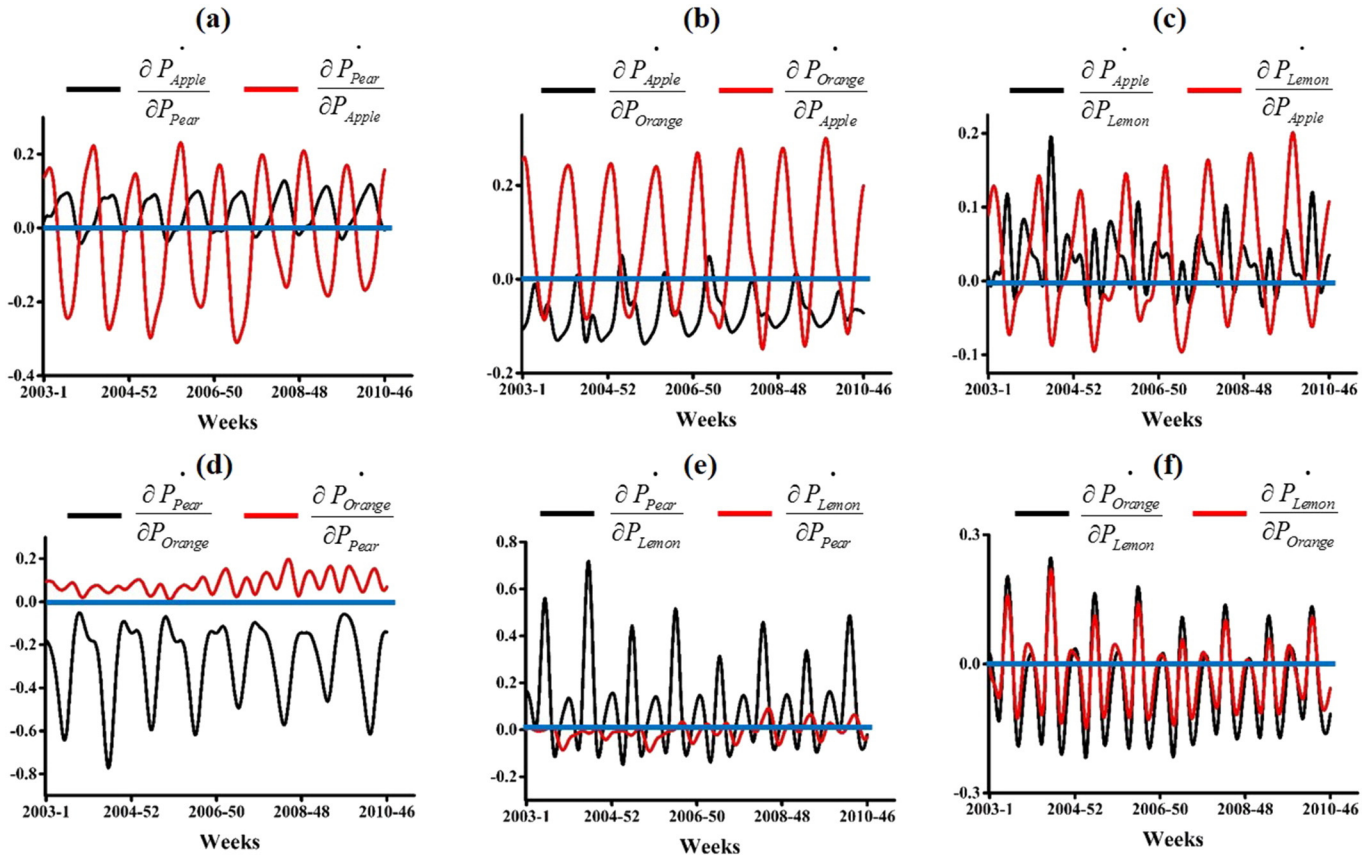

Fig. 6. Pairwise dynamic price interactions between: (a) apples and pears, (b) apples and oranges, (c) apples and lemons, (d) pears and oranges, (e) pears and lemons, and (f) oranges and lemons. The time (horizontal) axis shows year and week, e.g., 2003–1 denotes the first week of 2003. Empirically-detected endogenous volatility is driven by remarkably systematic simulated paired-price interactions that cycle annually. Apple and pear prices have a mutually beneficial relationship (meaning that an incremental increase in one has a positive impact on the growth rate of the other) in January and February of each year (when the cross derivatives are positive), and a predator (apple prices) – prey (pear prices) relationship the rest of the year (when the cross derivatives have opposite sign). Orange prices 'prey' on apple prices from approximately October to April each year, and a competitive relationship the rest of the years (when the cross derivatives turn negative). Apple prices 'prey' on lemon prices from about May to October each year, and the relationship turns 'symbiotic' over the remaining months. Orange prices 'prey' on pear prices, and pear prices 'prey' on lemon prices all year. Finally, orange and lemon prices are symbiotic in December and January and competitive the rest of the year.

cycling characterizing the empirical attractor. Third, the three-dimensional embedding space of the empirical market attractors reconstructed from observed data indicates that a minimum of at least three interacting prices is required to re-produce diagnosed market dynamics. Fourth, the phenomenological market model fit to price signals demonstrates that complex diagnosed dynamics can be reproduced by a nonlinear system of ODEs composed of second-order polynomial price interactions. A mechanistic market model for the study area need not include interactions more complex than this to successfully simulate diagnosed dynamics. Once a mechanistic market model has been specified, the approach outlined by Baker et al. (1996) to estimate coefficients in known dynamical systems can be applied.

Empirical evidence of nonlinear dynamic structure opens the door to true interdisciplinary mechanistic modeling. Most would agree that real-world food markets are integrated agricultural systems of climatic, environmental, economic, geopolitical and sociological processes whose interactions determine food production and consumption over time and space, and that many of these processes are not considered to be intrinsically random in their respective disciplines. Yet, the risk literature in agricultural economics relegates these processes to realm of 'real uncertainty'—generally interpreted to mean that agricultural decision-making environments are inherently uncertain due to uncontrollable and random exogenous events including weather, diseases, insect infestations, technological innovations, government policies, and so on (Feder 1979). In contrast, endogenous nonlinear explanations of observed complexity require that theory from economics and other disciplines be integrated—not relegated to random chance.

The diagnosis that the Italian organic fruit market studied is inherently unstable has important implications for food policy. First, this is evidence that this particular market cannot be relied upon as a 'natural corrective process' to stabilize observed price volatility. There may be scope for public intervention policies directed, for example, at increasing the flexibility of agricultural producers in responding to changing market conditions (Berg and Huffaker 2015). A source of inflexible response in EU organic fruit production is high sunk costs due to 'investment irreversibility' (Tzouramani et al. 2009). Sunk costs could be reduced by policies encouraging producers to replace highly-specialized with multi-purpose production facilities. Another source of inflexibility is that producers relying on bank financing for a major investment often require a period of financial consolidation before qualifying for a new loan. This 'investment' cycle could be smoothed by encouraging alternative financing options to bank loans such as equity capital provided by external investors (Berg and Huffaker 2015).

On a final note, one should be aware of important caveats to applying NLTS to the short and noisy data sets typically confronting food security volatility assessment. NLTS may fail to diagnose nonlinear dynamic structure in observed market data for several reasons (Williams 1997). First, real-world market dynamics in the study area may not evolve along a low-dimensional nonlinear attractor. Second, observed data may not lie on an existing real-world attractor. Finally, limited data may fail to adequately characterize an existing attractor. Faced with the short and noisy time-series data "one gives up the ambition of reconstructing the very fine structure of the real-world attractor including complex folding and fractal patterns …" (Vautard 1999). One

Table 5
Classification of pairwise price interactions.

Interactions	Jan	Feb	Mar	Apr	May	Jun	Jul	Aug	Sep	Oct	Nov	Dec
P_{apple}–P_{pear}												
Symbiotic	x	x										
Predator-prey[a]			x	x	x	x	x	x	x	x	x	x
Competitive												
P_{apple}–P_{orange}												
Symbiotic												
Predator-prey[b]	x	x	x	x						x	x	x
Competitive					x	x	x	x	x			
P_{apple}–P_{lemon}												
Symbiotic	x	x	x	x							x	x
Predator-prey[c]					x	x	x	x	x	x		
Competitive												
P_{pear}–P_{orange}												
Symbiotic												
Predator-prey[d]	x	x	x	x	x	x	x	x	x	x	x	x
Competitive												
P_{pear}–P_{lemon}												
Symbiotic												
Predator-prey[e]	x	x			x	x	x	x			x	x
Competitive			x	x					x	x		
P_{orange}–P_{lemon}												
Symbiotic	x											x
Predator-prey												
Competitive		x	x	x	x	x	x	x	x	x	x	

[a] *Predator* (P_{apple})–*Prey* (P_{pear}).
[b] *Predator* (P_{orange})–*Prey* (P_{apple}).
[c] *Predator* (P_{apple})–*Prey* (P_{lemon}).
[d] *Predator*(P_{orange})–*Prey*(P_{pear}).
[e] *Predator* (P_{pear})–*Prey* (P_{lemon}).

is limited to reconstructing a "sampling" or "skeleton" of a real-world attractor (Ghil et al. 2002), and cannot hope to recover "full dynamics … from a recording of a single variable" (Schreiber 1999). When nonlinear dynamic techniques fail, linear-stochastic approaches remain a viable alternative. However, we propose that NLTS diagnostics be applied before presuming linear-stochastic structures potentially falling short of real-world complexity.

6. Summary and concluding comments

Controversy over how to distinguish between endogenous and exogenous price volatility compromises the ability of governments and international agencies to assess the threat that volatility poses to food security, and to select suitable countermeasures. The root of the controversy is whether food-market dynamics normally stabilize exogenous

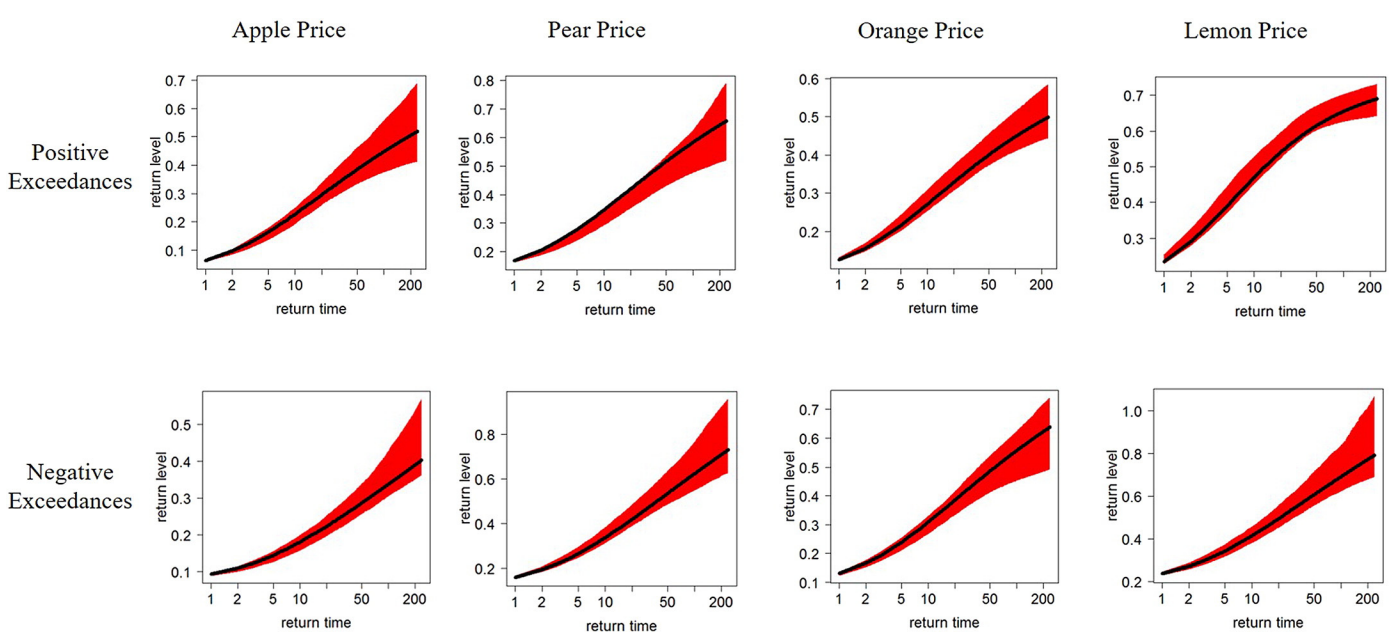

Fig. 7. Probabilistic modeling of exogenous volatility captured in the noise separated from each observed price anomaly. *Extreme Value Statistics* calculate the likelihood of extreme positive and negative noise levels exceeding selected thresholds, and produce 'return-level' plots (log scale) estimating the times expected ('return times') before positive and negative exceedances of increasing magnitudes ('return levels') are realized. Red bands are 95% bootstrapped pointwise confidence intervals. (For interpretation of the references to color in this figure legend, the reader is referred to the web version of this article.)

Please cite this article as: Huffaker, R., et al., Distinguishing between endogenous and exogenous price volatility in food security assessment: An empirical nonlinear dynamics appr..., Agricultural Systems (2016), http://dx.doi.org/10.1016/j.agsy.2016.09.019

Table 6
Threshold values for extreme value statistics.[a]

	Positive noise	Negative noise
Apple prices		
Threshold	0.05 (€/kg)	0.08 (€/kg)
Exceedances	115	126
Weekly rate	0.27	0.3
Pear prices		
Threshold	0.15 (€/kg)	0.13 (€/kg)
Exceedances	118	126
Weekly rate	0.28	0.3
Orange prices		
Threshold	0.1 (€/kg)	0.1 (€/kg)
Exceedances	126	126
Weekly rate	0.3	0.3
Lemon prices		
Threshold	0.18 (€/kg)	0.2 (€/kg)
Exceedances	128	132
Weekly rate	0.3	0.31

[a] Observed time series converted to anomalies from the mean.

random shocks or endogenously destabilize prices. Since, neither viewpoint is a theoretical imperative, assessing market dynamics becomes an empirical issue.

We proposed an empirical framework—based on nonlinear dynamics—to test for endogenous market dynamics in organic apple, pear, orange, and lemon prices at the Milano (Italy) Ipercoop. Results indicate that long-term market dynamics are deterministic, nonlinear and low dimensional. Observed price volatility is endogenous to inherently unstable market behavior, and food policy looking to ease volatility cannot rely on the market to stabilize prices in the face of exogenous shocks.

Diagnosed real-world dynamic market structure was successfully simulated with a parsimonious phenomenological model formulated as a deterministic system of ordinary differential equations with second-order polynomial price interactions. We indicated how diagnosed dynamics and phenomenological modeling would inform future mechanistic modeling attempting to provide theoretical explanations for endogenous price volatility.

Our proposed diagnostic scheme cannot be expected to diagnose low-dimensional nonlinear dynamic market structure in all applications—the real-world market dynamics under investigation may not evolve along a low-dimensional attractor, or the data may be too limited to provide an adequate sampling of an existing attractor. However, we conclude that nonlinear diagnostics represent a valuable opportunity to glean highly useful information for food security assessment in a mathematically- and statistically-rigorous manner.

Table 7
Noise return times and levels.[a]

Return times	Apple prices	Pear prices	Orange prices	Lemon prices
Return levels (positive exceedances)				
5 weeks	0.095	0.22	0.18	0.34
26 weeks	0.31	0.31	0.27	0.48
53 weeks	0.39	0.39	0.34	0.57
Return levels (negative exceedances)				
5 weeks	0.12	0.22	0.19	0.3
26 weeks	0.17	0.33	0.29	0.4
53 weeks	0.22	0.44	0.38	0.5

[a] Observed time series converted to anomalies from the mean.

Acknowledgements

RH acknowledges support from NIFA.

References

Adrangi, B., Chatrath, A., 2003. Nonlinear dynamics in futures prices: evidence from the coffee, sugar and cocoa exchange. Appl. Financ. Econ. 13, 245–256.
Baker, G., Gollub, J., Blackburn, J., 1996. Inverting chaos: extracting system parameters from experimental data. Chaos 6, 528–533.
Berg, E., Huffaker, R., 2015. Economic dynamics of the German hog-price cycle. Int. J. Food Syst. Dyn. 6, 64–80.
Brown, T., 1996. Measuring chaos using the Lyapunov exponent. In: Kiel, E., Elliott, E. (Eds.), Chaos Theory in the Social Sciences: Foundations and Applications. University of Michigan, Michigan, pp. 53–66.
Cafiero, C., Bobenrieth, E.S.A., Bobenrieth, J.R.A., Wright, B., 2011. The empirical relevance of the competitive storage model. J. Econ. 162, 44–54.
Canavari, M., Olson, K., 2007. Current issues in organic Food: Italy. In: Canavari, M., Olson, K. (Eds.), Organic Food: Consumers' Choices and Farmers' Opportunities. Springer, New York, pp. 171–183.
Canavari, M., Bazzani, G., Spadoni, R., Regazzi, D., 2002. Food safety and organic fruit demand in Italy: a survey. Br. Food J. 104, 220–232.
Chatrath, A., Adrangi, B., Kanwalroop, K., 2000. Are commodity prices chaotic? Agric. Econ. 27, 123–137.
Chavas, J.P., Holt, M., 1993. Market instability and nonlinear dynamics. Am. J. Agric. Econ. 75, 113–120.
Clark, A., 2014. MultispatialCCM: Multispatial Convergent Cross Mapping. Retrieved from https://cran.r-project.org/package=multispatialCCM.
Constantine, W., Percival, D., 2014. Fractal: Fractal Time Series Modeling and Analysis. Retrieved from https://cran.r-project.org/package=fractal.
Csardi, G., Nepusz, T., 2006. The Igraph Software Package for Complex Network Research. Retrieved from https://igraph.org.
Deaton, A., Laroque, G., 1996. Competitive storage and commodity price dynamics. J. Polit. Econ. 104, 896–923.
Di Narzo, A., Di Narzo, F., 2013. TseriesChaos: Analysis of Nonlinear Time Series. Retrieved from https://cran.r-project.org/package=tseriesChaos.
Dieci, R., Westerhoff, F., 2009. Stability analysis of a cobweb model with market interactions. Appl. Math. Comput. 215, 2011–2023.
Elsner, J., Tsonsis, A., 2010. Singular Spectrum Analysis. Plenum Press, New York.
Feder, G., 1979. Pesticides, information, and pest management under uncertainty. Am. J. Agric. Econ. 61, 97–103.
G20, 2011. Ministerial Declaration: Action Plan on Food Price Volatility and Agriculture, Meeting of G20 Agicultural Ministiers, Paris.
Galtier, F., 2013. Managing food price instability: Critical assessment of the dominant doctrine. Glob. Food Sec. 2, 72–81.
Garcia, C., 2015. NonlinearTseries: Nonlinear Time Series Analysis. Retrieved from https://cran.r-project.org/package=nonlinearTseries.
Ghil, M., Allen, M., Dettinger, M., Ide, K., Kondrashov, D., Mann, M., Robertson, A., Saunders, A., Tian, Y., Varadi, F., Yiou, P., 2002. Advanced spectral methods for climatic time series. Rev. Geophys. 40, 1–41.
Gilleland, E., 2015. R Package ExtRemes. Available: http://www.assessment.ucar.edu/toolkit/ (Accessed 2016 Jan 2).
Gilleland, E., Katz, R., 2011. New software to analyze how extremes change over time. Eos 92, 13–14.
Glendinning, P., 1994. Stability, Instability and Chaos: An Introduction to the Theory of Nonlinear Differential Equations. Cambridge University Press, Cambridge, UK.
Golyandina, N., Korobeynikov, A., 2014. Basic singular spectrum analysis and forecasting with R. Comput. Stat. Data Anal. 71, 934–954.
Golyandina, N., Nekrutkin, V., Zhigljavsky, A., 2001. Analysis of Time Series Structure. Chapman & Hall/CRC, New York.
Gouel, C., 2012. Agricultural price instability: a survey of competing explanations and remedies. J. Econ. Surv. 26, 129–156.
Guerra, E.V.A., Bobenrieth, E.S.A., Bobenrieth, J.R.A., Cafiero, C., 2015. Emprical commodity storage model: the challenge of matching data and theory. Eur. Rev. Agric. Econ. 42, 607–623.
Hastings, A., 1978. Global stability of two species systems. J. Math. Biol. 5, 399–403.
HLPE, 2011. Price Volatility and Food Security, a Report by the High Level Panel of Experts on Food Security and Nutrition of the Committee on World Food Security, Rome.
Hommes, C., 1991. Adaptive learning and roads to chaos. Econ. Lett. 36, 127–132.
Hornberger, G., Spear, R., 1981. An approach to the preliminary analysis of environmental systems. J. Environ. Manag. 12, 7–18.
Jensen, R., Urban, R., 1984. Chaotic price behavior in a non-linear cobweb model. Econ. Lett. 15, 235–240.
Kalkuhl, M., Kornher, L., Kozicka, M., Boulanger, P., Torero, M., 2013. Conceptural Framework on Price Volatility and Its Impact on Food and Nutrition Security in the Short Term. FOODSECURE, European Union Seventh Framework Programme.
Kantz, H., Schreiber, T., 1997. Nonlinear Time Series Anaysis. Cambridge University Press, Cambridge.
Kaplan, D., Glass, L., 1995. Understanding Nonlinear Dynamics. Springer, New York.
Katz, R., 2010. Statistics of extremes in climate change. Clim. Chang. 100, 71–76.
Kot, M., Schaffer, W., Truty, G., Graser, D., Olsen, L., 1988. Changing criteria for imposing order. Ecological Modeling 43, 75–110.
Kugiumtzis, D., 1999. Test your surrogate data before you test for nonlinearity. Phys. Rev. E 60, 2808–2816.

Mevik, B., Wehrens, R., 2007. The pls package: principal component and partial least squares regression in R. J. Stat. Softw. 18, 1–24.
Nicholson, C., Stephensen, M., 2015. Milk price cycles in the U.S. dairy supply chain and their management implications. Agribusiness http://dx.doi.org/10.1002/agr.21416.
Oreskes, N., Shrader-Frechette, K., Belitz, K., 1994. Verification, validation, and confirmation of numerical models in the earth sciences. Science 263, 641–646.
Ritter, A., Muñoz-Carpena, R., 2013. Performance evaluation of hydrologic models: statistical significance for reducing subjectivity in goodness-of-fit assessments. J. Hydrol. 480, 33–45.
Rykiel, E., 1996. Testing ecological models: the meaning of validation. Ecol. Model. 90, 229–244.
Saltelli, A., Funtowitz, S., 2014. When all models are wrong. Comput. Model. Winter 79–85.
Schreiber, T., 1999. Interdiciplinary application of nonlinear time series methods. Phys. Rep. 308, 1–64.
Schreiber, T., Schmitz, A., 2000. Surrogate time series. Phys. D 142, 346–382.
Small, M., Tse, C., 2002. Applying the method of surrogate data to cyclic time series. Phys. D 164, 187–201.
Small, M., Tse, C., 2003. Detecting determinism in time series: the method of surrogate data. IEEE Trans. Circuits Syst. 50, 663–672.
Soetaert, K., Petzoldt, T., Setzer, R., 2015. Solving differential equations in R: package deSolve. J. Stat. Softw. 39, 1–25.
Sprott, J., 2003. Chaos and Time Series Analysis. Oxford University Press, Oxford.
Strogatz, S., 1994. Nonlinear Dynamics and Chaos. Addison-Wesley Publishing Company, New York.
Sugihara, G., May, R., Hao, Y., Chih-hao, H., Deyle, E., Fogarty, M., Munch, S., 2012. Detecting causality in complex ecosystems. Science 338, 496–500.
Takens, F., 1980. In: Rand, D., Young, L. (Eds.), Detecting strange attractors in turbulence. Dynamical Systems and Turbulence Springer, New York, pp. 366–381.
Theiler, J., Eubank, S., Longtin, A., Galdrikian, B., Farmer, J., 1992. Testing for nonlinearity in time series: the method of surrogate data. Phys. D 58, 77–94.
Tzouramani, I., Liontakis, A., Sintori, A., Alexopoulos, G., 2009. Policy Implementations for Organic Agricultural: A Real Options Approach, The 83rd Annual Conference of the Agricultural Economics Society. Dublin, Ireland.
Vautard, R., 1999. Patterns in time: SSA and MSSA in analysis of climate. In: von Storch, H., Navarra, A. (Eds.), Analysis of Climate Variability. Springer.
Wei-Dong, L., Ren, K., Meunier-Guttin-Cluzel, S., Gouesbet, G., 2003. Global vector-field reconstruction of nonlinear dynamical systems from a time series with SVD method and validation with Lyapunov exponents. Chin. Phys. 12, 1366–1373.
Williams, G., 1997. Chaos Theory Tamed. John Henry Press, Washington D.C.
Zachilas, L., Gkana, A., 2011. Nonlinear supply and demand model with two interrelated markets. J. Eng. Sci. Technol. Rev. 3, 227–232.

Please cite this article as: Huffaker, R., et al., Distinguishing between endogenous and exogenous price volatility in food security assessment: An empirical nonlinear dynamics appr..., Agricultural Systems (2016), http://dx.doi.org/10.1016/j.agsy.2016.09.019